Supporting Information

Constructing a brand-new advanced oxidation process system comprised of MgO_2 nanoparticles and MgNCN/MgO nanocomposites for organic pollutant degradation

Ningning Dong [a], Doudou Wu [a], Lifa Ge [a], Wei Wang [a, *], Fatang Tan [a], Xinyun Wang [a], Xueliang Qiao [a] and Po Keung Wong [b]

[a] *State Key Laboratory of Materials Processing and Die & Mould Technology, School of Materials Science and Engineering, Huazhong University of Science and Technology, Wuhan 430074, Hubei, China*

[b] *School of Life Sciences, The Chinese University of Hong Kong, Shatin, NT, Hong Kong SAR, China*

* Corresponding author:

Wei Wang, Tel/fax: +86-27-87541540, E-mail: weiwang@hust.edu.cn

Preparation of individual MgNCN and MgO

MgNCN nanoparticles were prepared by calcining the mixture of thiourea and $(MgCO_3)_4{\cdot}Mg(OH)_2{\cdot}5H_2O$. Typically, 1.00 g of thiourea and 0.33 g of $(MgCO_3)_4{\cdot}Mg(OH)_2{\cdot}5H_2O$ were mixed evenly in a agate mortar and the homogeneous mixture was transferred into a crucible. Subsequently, the crucible was covered with a lid and aluminum foil, and then heated from room temperature to 550 °C with a heating rate of 10 °C/min and kept at 550 °C for another 2 h in a muffle furnace. Finally, pure-phased MgNCN was obtained after cooling to room temperature. MgO was prepared by calcining $(MgCO_3)_4{\cdot}Mg(OH)_2{\cdot}5H_2O$ alone followed the same procedure.

Degradation kinetics

The pseudo-first order (Eq. 1) and pseudo-second order (Eq. 2) models were used to study the kinetics of MB degradation in the MgO_2-MgNCN/MgO system under different conditions including the MgO_2 dosage, MgNCN/MgO dosage, initial solution pH and degradation temperature.

Pseudo-first order: $$ln\frac{C_t}{C_0} = -k_1 t \quad (1)$$

Pseudo-second order: $$\frac{1}{C_0} - \frac{1}{C_t} = k_2 t \quad (2)$$

Where k_1 (h^{-1}) and k_2 (L mg^{-1} h^{-1}) are reaction rate constants of the pseudo-first-order and pseudo-second-order models, respectively. C_0 (mg/L) is the initial concentration of MB solution, while C_t (mg/L) is the concentration of MB at the certain time t (h).

Slow-release test of MgO_2

It was well known that MgO_2 could slowly react with H_2O to release H_2O_2 (Eq. 3). The slow-release ability of MgO_2 in aqueous solution was determined by the concentration of released H_2O_2 in aqueous solution using a standard solution of potassium permanganate ($KMnO_4$). Specifically, 60 mg of MgO_2 was added into 300 mL of water under continuous stirring. At given time intervals, 15 mL of suspension was taken out and immediately filtered to remove solid particles. The released H_2O_2 concentration in the filtrate was quantitatively evaluated using the permanganate (0.4 mM) titration method (Eq. 4).

$$MgO_2 + 2H_2O \rightarrow Mg(OH)_2 + H_2O_2 \quad (3)$$

$$2KMnO_4 + 5H_2O_2 + 3H_2SO_4 \rightarrow K_2SO_4 + 2MnSO_4 + 5O_2\uparrow + 8H_2O \quad (4)$$

Oxidant utilization efficiency

To evaluate the utilization efficiency of MgO_2, 20 mg of MgO_2 nanoparticles and 10 mg of MgNCN/MgO nanocomposites were used to continuously degrade 10 mg/L MB until MB was no longer degraded. Then, the utilization efficiency of MgO_2 was obtained according to the reported method.[1] Similarly, the utilization efficiencies of common H_2O_2 and CaO_2 (equimolar active oxygen to MgO_2), activated by MgNCN/MgO (10 mg) and Fe^{2+} (46 mg of $FeSO_4 \cdot 7H_2O$), were estimated for comparisons. Considering the difference in oxidant purity, the utilization efficiencies of oxidants were calculated based on their active oxygen content.

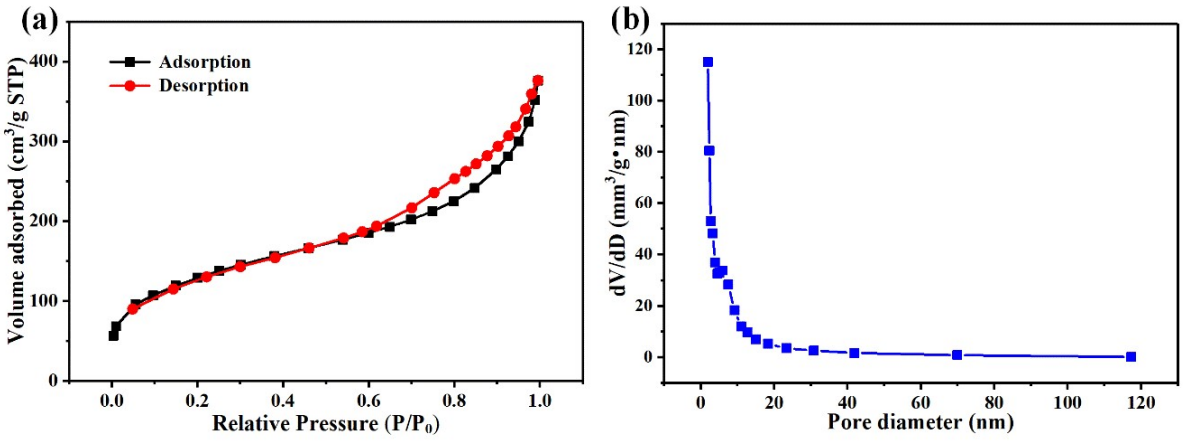

Figure S1. N_2 adsorption/desorption isotherms (a) and pore-size distribution (b) of MgO_2 nanoparticles.

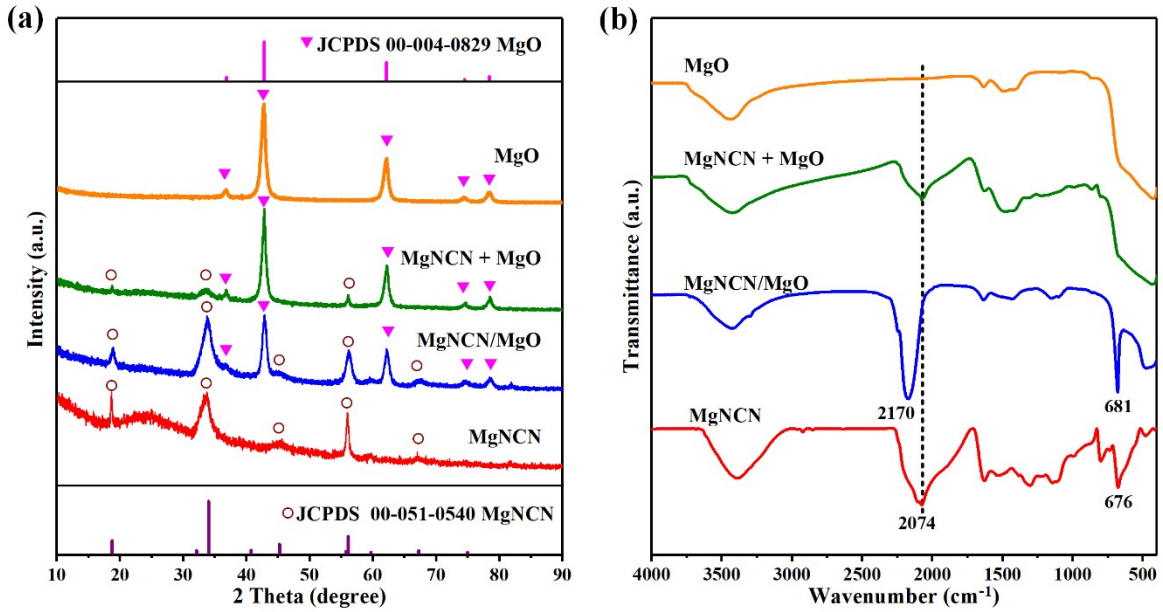

Figure S2. XRD patterns (a), FTIR spectra (b) of MgNCN, MgO, MgNCN/MgO nanocomposites and the physical mixture of MgNCN and MgO with mass ratio of 1:1.

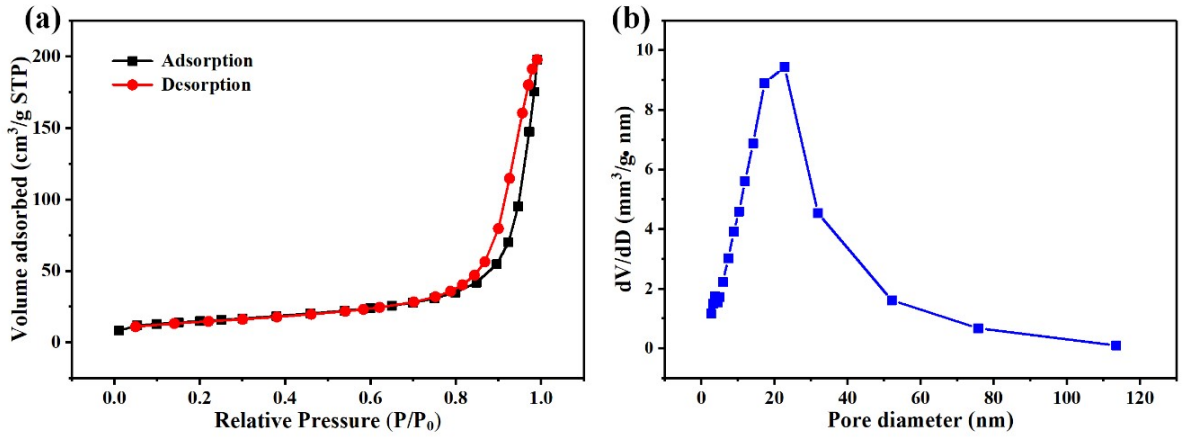

Figure S3. N_2 adsorption/desorption isotherms (a) and pore-size distribution (b) of MgNCN/MgO nanocomposites.

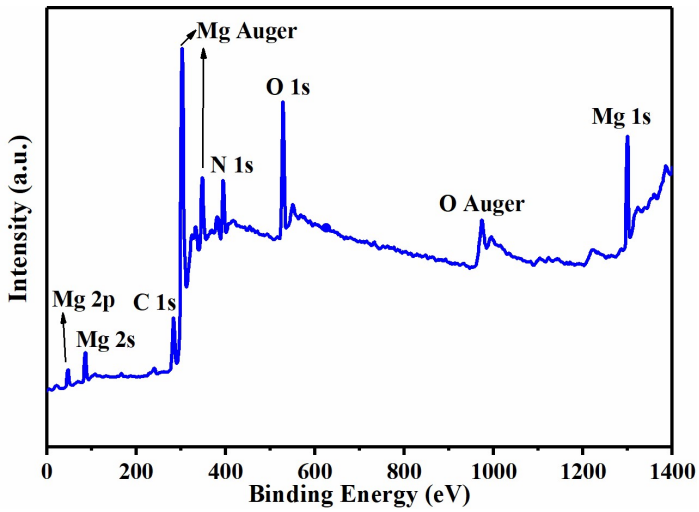

Figure S4. Survey XPS spectrum of MgNCN/MgO nanocomposites.

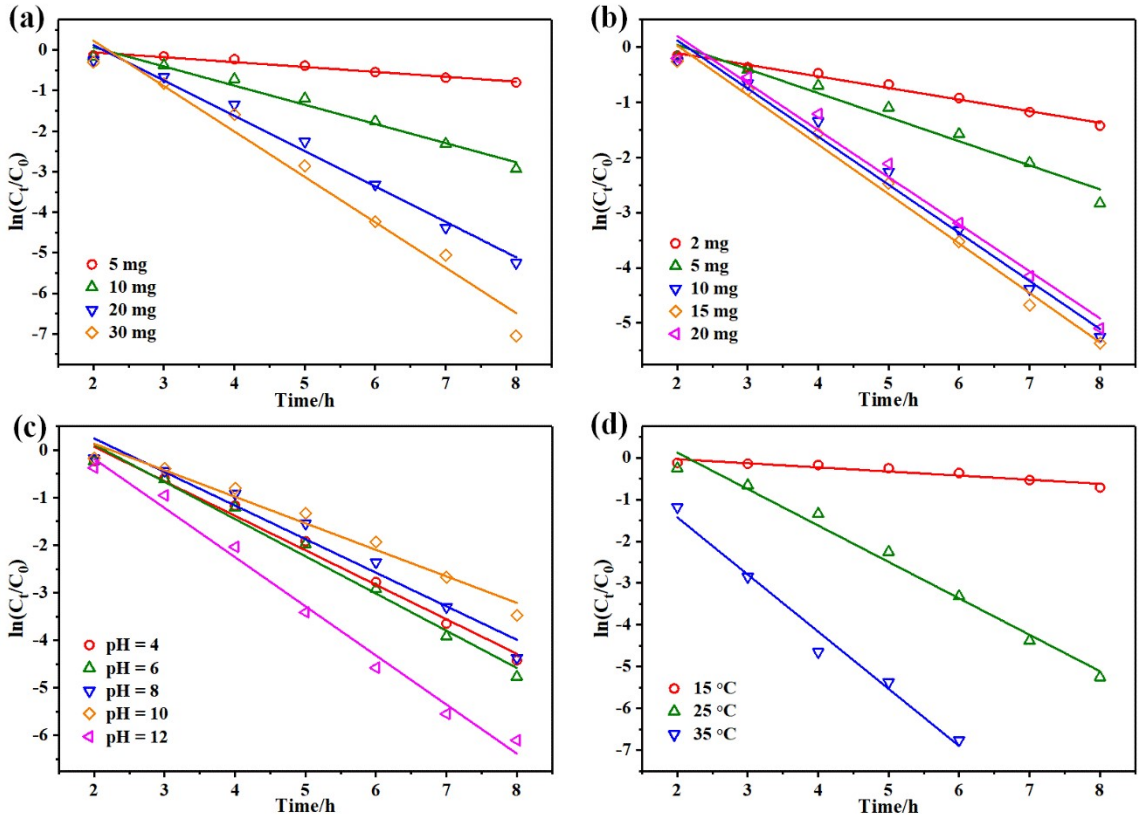

Figure S5. Pseudo-first-order kinetic curves of MB degradation under different conditions: MgO_2 dosage (a), MgNCN/MgO dosage (b), initial solution pH (c), and degradation temperature (d).

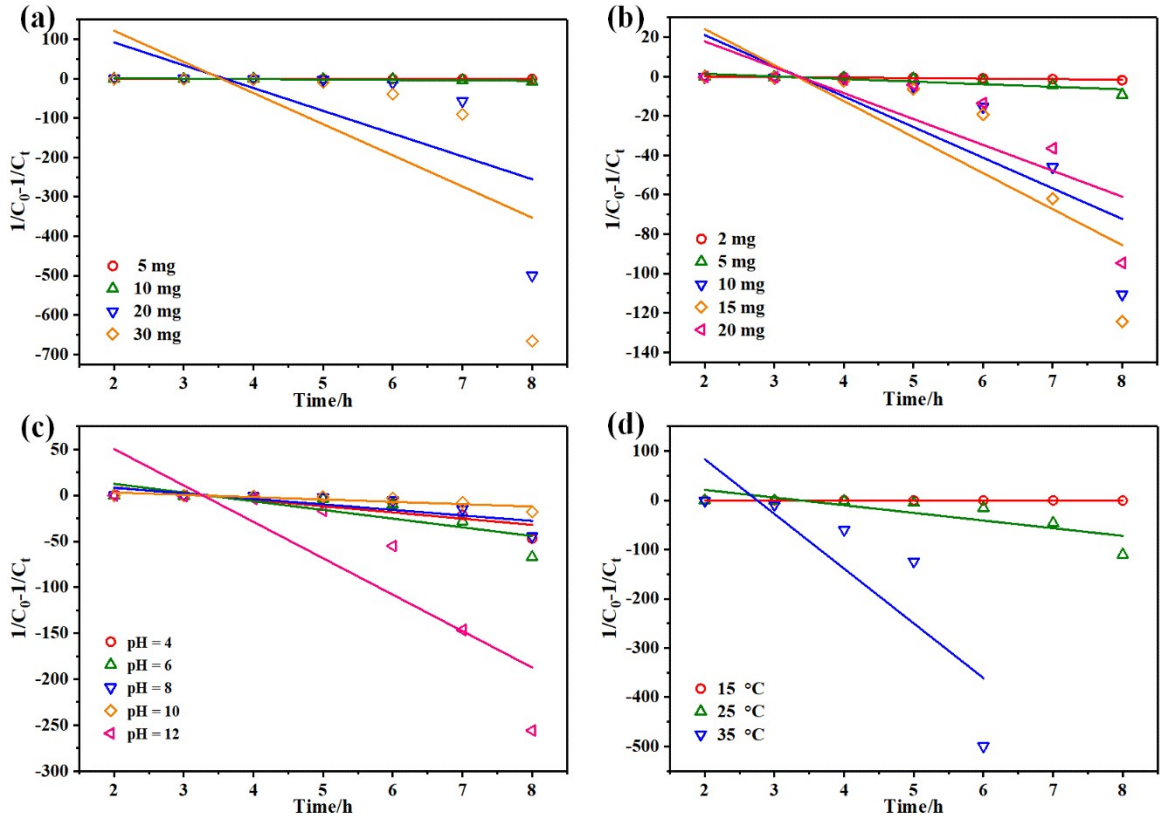

Figure S6. Pseudo-second-order kinetic curves of MB degradation under different conditions: MgO_2 dosage (a), MgNCN/MgO dosage (b), initial solution pH (c), and degradation temperature (d).

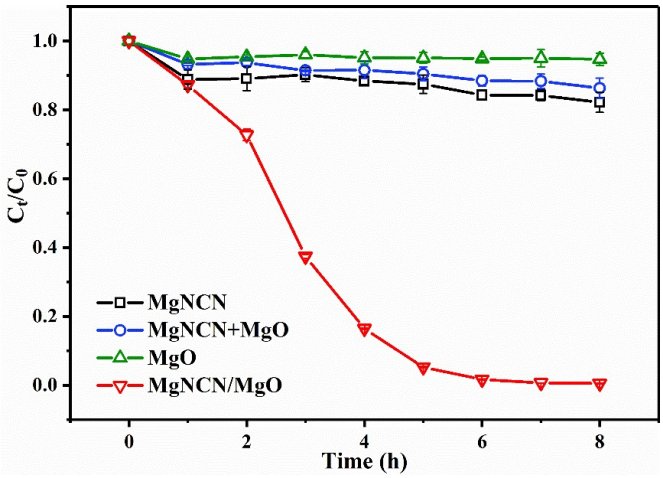

Figure S7. Comparative experiments of MB degradation with different activators (Reaction conditions：100 mL of 10 mg/L MB, 20 mg of MgO_2, 10 mg of activator).

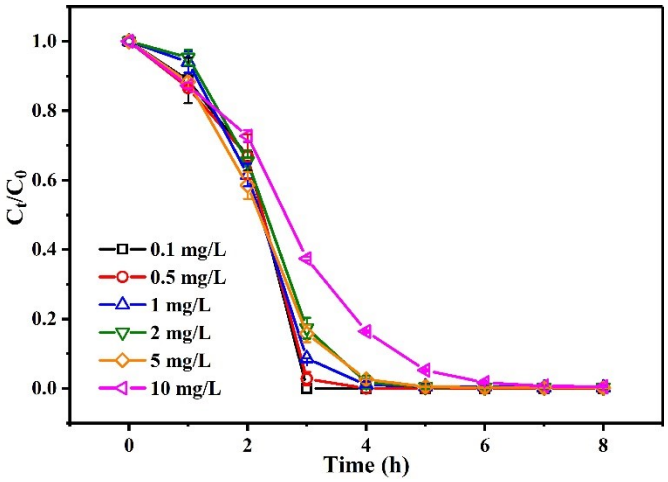

Figure S8. Effects of initial MB concentration on MB degradation (Reaction conditions: 100 mL of MB solution, 20 mg of MgO_2, 10 mg of MgNCN/MgO).

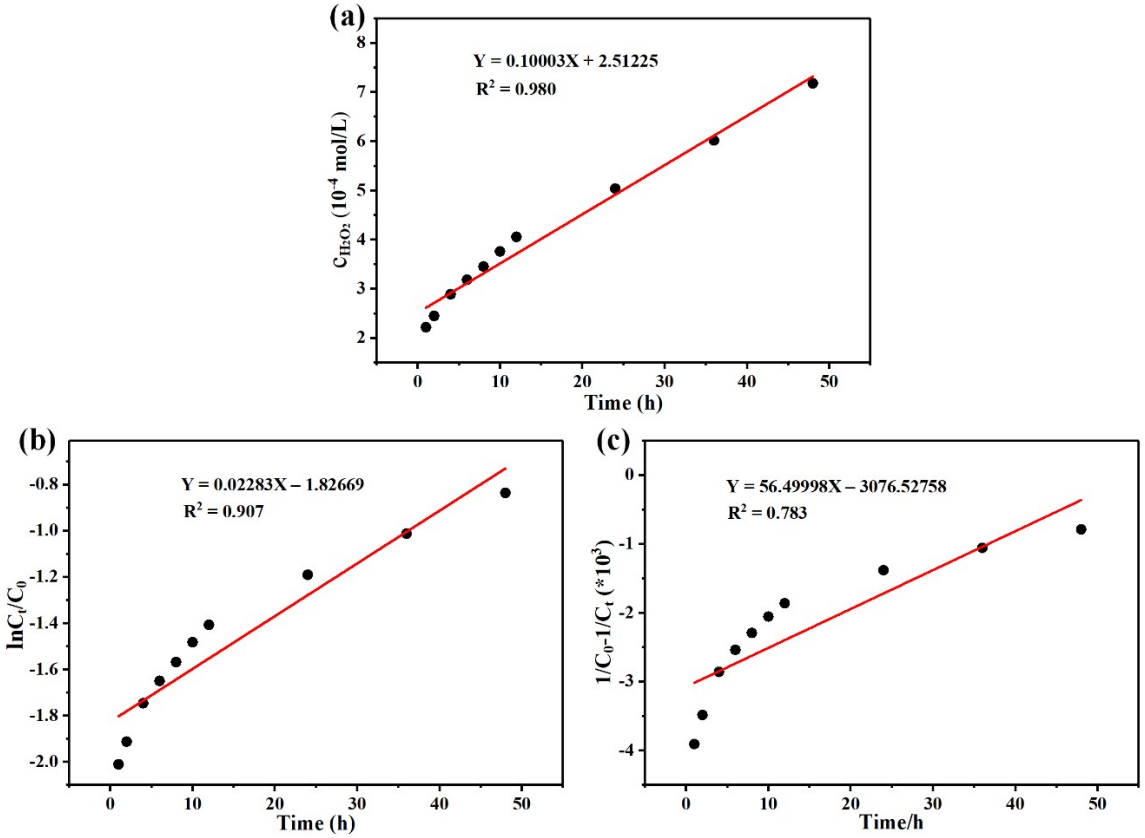

Figure S9. Linear curves fitted by pseudo-zero-order kinetic (a), pseudo-first-order kinetic (b) and pseudo-second-order kinetic (c) models for the H_2O_2 release from MgO_2.

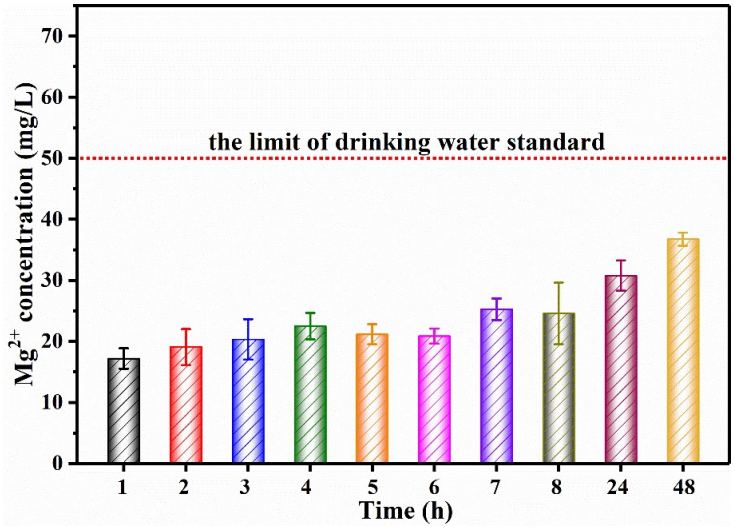

Figure S10. Mg^{2+} concentrations released from the MgO_2-MgNCN/MgO system (Reaction conditions: 100 mL of 10 mg/L MB, 20 mg of MgO_2, 10 mg of MgNCN/MgO).

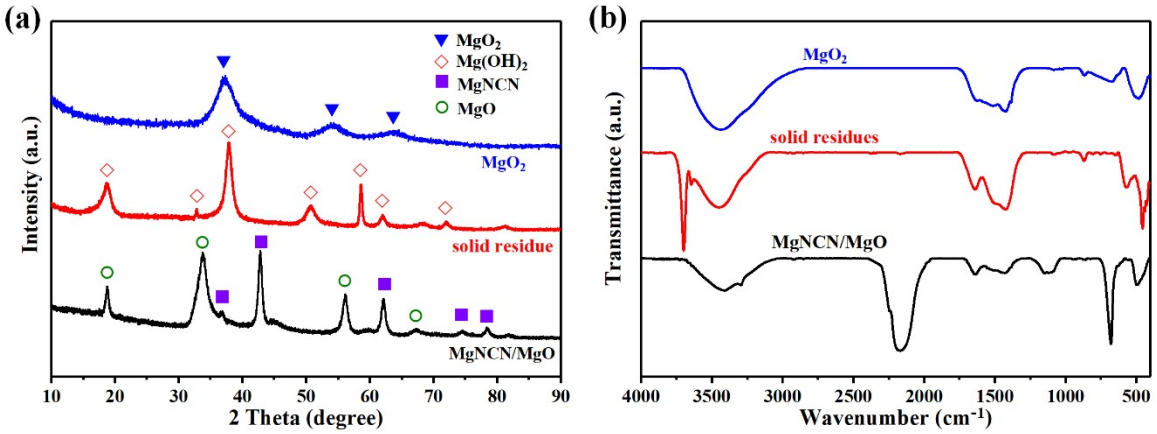

Figure S11. XRD patterns (a) and FTIR spectra (b) of MgO_2, MgNCN/MgO and solid residue after 5 runs of MB degradation.

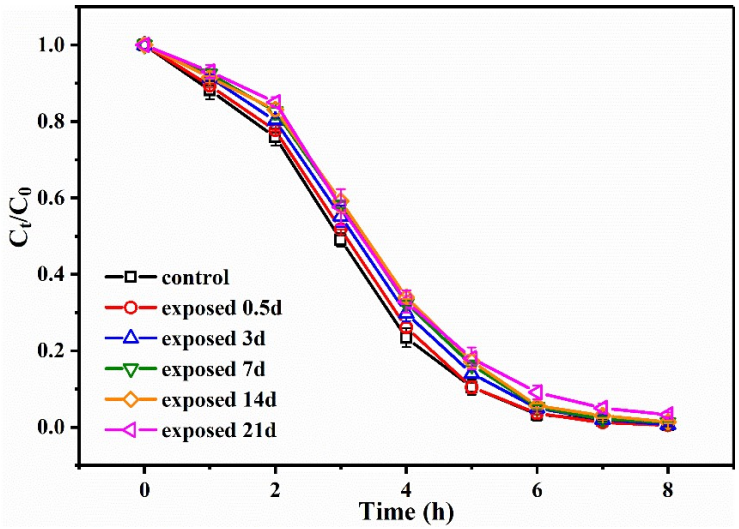

Figure S12. Effect of exposure time of MgO_2 on MB degradation (Reaction conditions:100 mL of 10 mg/L MB, 20 mg of MgO_2 with different exposure time, 10 mg of MgNCN/MgO).

Table S1. Kinetic parameters of MB degradation in the MgO_2-MgNCN/MgO system under different conditions

Parameters		Pseudo-first order model		Pseudo-second order model	
		$K_1(h^{-1})$	R_1^2	K_2 (L mg^{-1} h^{-1})	R_2^2
MgO_2 dosage (mg)	5	0.120	0.969	0.110	0.949
	10	0.473	0.979	1.092	0.726
	20	0.872	0.985	57.871	0.455
	30	1.120	0.974	79.071	0.486
MgNCN/MgO dosage (mg)	2	0.210	0.988	0.279	0.928
	5	0.437	0.967	1.315	0.748
	10	0.872	0.985	15.558	0.678
	15	0.897	0.990	18.295	0.714
	20	0.853	0.983	13.135	0.667
Initial solution pH	4	0.725	0.986	6.782	0.719
	6	0.783	0.982	9.459	0.687
	8	0.706	0.963	5.995	0.634
	10	0.558	0.971	2.540	0.716
	12	1.033	0.988	39.616	0.765
T (°C)	15	0.098	0.903	0.085	0.861
	25	0.872	0.985	15.558	0.678
	35	1.368	0.982	111.117	0.717

Table S2. Comparison of the capacities of other AOP systems for MB degradation.

Degradation system	Catalyst (g/L)	Oxidant (mM)	MB (mg/L)	pH range	Degradation efficiency (%)	References
MgO_2+MgNCN/MgO	0.1	3.6	10	4-12	>98	This work
H_2O_2+FePC	0.5	1	100	2-5	>90	2
H_2O_2+MPCMSs+ NH_2OH	2	16	40	3.1-9.6	>40	3
H_2O_2+Fe_3O_4@MnO_2	0.3	30	40	2-9	>30	4
H_2O_2+Fe_2GeS_4	0.3	50	20	3-11	>40	5
H_2O_2+g-C_3N_4/CDs/Fe(II)	0.5	1	60	3-9	>60	6
H_2O_2+Nb_2O_5	1	441.2	37.5	5	100	7
H_2O_2+PCN-250 (Fe2Mn)	0.5	4000	15	natural	100	8
MgO_2+$Fe_2(SO_4)_3 \cdot xH_2O$	0.1	0.9	20	2-10	>90	9
PMS+BC-CuO	0.2	2	37.4	3-11	>80	10
PMS+Elbaite	1	0.7	5	2-12	>30	11

Table S3. Water quality of tap water.

No.	Substance	Concentration
1	Ammonia nitrogen (mg/L）	□0.02
2	Cyanogen chloride (mg/L）	□0.01
3	Atrazine (mg/L）	□0.0001
4	1.2-dichlorobenzene (mg/L）	□0.001
5	Chlorobenzene (mg/L）	□0.001
6	α-1,2,3,4,5,6-Hexachlorocyclohexane (μg/L)	≤ 0.000002
7	Parathion (mg/L）	□0.001
8	2,4,6-trichlorophenol (mg/L）	□0.0005

Table S4. Water quality of different types of surface water.

No.	Surface water / Standard value / Project	Yangtze River	East lake and Han River	Moon lake
1	pH	6 ～ 9		
2	Dissolved oxygen ≥	6	5	3
3	Permanganate Index (mg/L) ≤	4	6	10
4	COD (mg/L) ≤	15	20	30
5	BOD_5 (mg/L) ≤	3	4	6
6	NH_3-N (mg/L) ≤	0.5	1.0	1.5
7	Total phosphorus (mg/L) ≤	0.1	0.2	0.3
8	Total nitrogen (mg/L) ≤	0.5	1.0	1.5
9	Cu (mg/L) ≤	1.0	1.0	1.0
10	Zn (mg/L) ≤	1.0	1.0	2.0
11	F^- (mg/L) ≤	1.0	1.0	1.5
12	Se (mg/L) ≤	0.01	0.01	0.02
13	As (mg/L) ≤	0.05	0.05	0.1
14	Hg (mg/L) ≤	0.00005	0.0001	0.001
15	Cd (mg/L) ≤	0.005	0.005	0.005
16	Cr^{6+} (mg/L) ≤	0.05	0.05	0.05
17	Pb (mg/L) ≤	0.01	0.05	0.05
18	Cyanide (mg/L) ≤	0.05	0.2	0.2
19	Volatile Phenol (mg/L) ≤	0.002	0.005	0.01
20	Petroleum (mg/L) ≤	0.05	0.05	0.5
21	Anionic Surfactant (mg/L) ≤	0.2	0.2	0.3
22	Sulfide (mg/L) ≤	0.1	0.2	0.5
23	Fecal coliforms (CFU/L) ≤	2000	10000	20000

References

1. X. Yang, J. Cai, X. Wang, Y. Li, Z. Wu, W. D. Wu, X. D. Chen, J. Sun, S. P. Sun and Z. Wang, A bimetallic Fe-Mn oxide-activated oxone for in situ chemical oxidation (ISCO) of trichloroethylene in groundwater: efficiency, sustained activity, and mechanism investigation, *Environ. Sci. Technol.*, 2020, **54**, 3714-3724.
2. C. Ma, S. Feng, J. Zhou, R. Chen, Y. Wei, H. Liu and S. Wang, Enhancement of H_2O_2 decomposition efficiency by the co-catalytic effect of iron phosphide on the Fenton reaction for the degradation of methylene blue, *Appl. Catal. B: Environ.*, 2019, **259**, 118015.
3. L. Zhou, Y. Shao, J. Liu, Z. Ye, H. Zhang, J. Ma, Y. Jia, W. Gao and Y. Li, Preparation and characterization of magnetic porous carbon microspheres for removal of methylene blue by a heterogeneous Fenton reaction, *ACS Appl. Mater. Interfaces*, 2014, **6**, 7275-7285.
4. L. Wolski, A. Walkowiak and M. Ziolek, Formation of reactive oxygen species upon interaction of Au/ZnO with H_2O_2 and their activity in methylene blue degradation, *Catal. Today*, 2019, **333**, 54-62.
5. X. Shi, A. Tian, J. You, H. Yang, Y. Wang and X. Xue, Degradation of organic dyes by a new heterogeneous Fenton reagent-Fe_2GeS_4 nanoparticle, *J. Hazard. Mater.*, 2018, **353**, 182-189.
6. X. Li, Y. Pi, L. Wu, Q. Xia, J. Wu, Z. Li and J. Xiao, Facilitation of the visible light-induced Fenton-like excitation of H_2O_2 via heterojunction of g-C_3N_4/NH_2-Iron terephthalate metal-organic framework for MB degradation, *Appl. Catal. B: Environ.*, 2017, **202**, 653-663.
7. L. Wolski and M. Ziolek, Insight into pathways of methylene blue degradation with H_2O_2 over mono and bimetallic Nb, Zn oxides, *Appl. Catal. B: Environ.*, 2018, **224**, 634-647.
8. A. Kirchon, P. Zhang, J. Li, E. A. Joseph, W. Chen and H. C. Zhou, Effect of isomorphic metal substitution on the Fenton and photo-Fenton degradation of methylene blue using Fe-based metal-organic frameworks, *ACS Appl. Mater. Interfaces*, 2020, **12**, 9292-9299.
9. D. Wu, Y. Bai, W. Wang, H. Xia, F. Tan, S. Zhang, B. Su, X. Wang, X. Qiao and P. K. Wong, Highly pure MgO_2 nanoparticles as robust solid oxidant for enhanced Fenton-like degradation of organic contaminants, *J. Hazard. Mater.*, 2019, **374**, 319-328.

10. Z. Li, D. Liu, W. Huang, X. Wei and W. Huang, Biochar supported CuO composites used as an efficient peroxymonosulfate activator for highly saline organic wastewater treatment, *Sci. Total Environ*., 2020, **721**, 137764.
11. C. Yu, M. Wen, S. Li, Z. Tong, Y. Yin, X. Liu, Y. Li, Z. Wu and D. D. Dionysiou, Elbaite catalyze peroxymonosulfate for advanced oxidation of organic pollutants: Hydroxyl groups induced generation of reactive oxygen species, *J. Hazard. Mater.*, 2020, **398**, 122932.